Biochemistry and Biophysics Reports 39 (2024) 101781

Contents lists available at ScienceDirect

Biochemistry and Biophysics Reports

journal homepage: www.elsevier.com/locate/bbrep

Proteasome and PARP1 dual-target inhibitor for multiple myeloma: Fluzoparib

Kai Deng [a], Qiongqiong Li [b], Lina Lu [b], Luting Wang [b], Zhiyong Cheng [c], Suyun Wang [b,*]

[a] Department of Orthopedics, Shenzhen Longhua District Central Hospital, Shenzhen, Guangdong, China
[b] Department of Hematology, Shenzhen Longhua District Central Hospital, Shenzhen, Guangdong, China
[c] Department of Hematology, Baoding No.1 Hospital, Baoding, Hebei, China

ARTICLE INFO

Keywords:
Computer-aided drug discovery
Fluzoparib
Multi-target drug
Multiple myeloma
Poly(ADP-Ribose) polymerase

ABSTRACT

One of the current mainstream treatments for multiple myeloma (MM) is chemotherapy. However, due to the high clonal heterogeneity and genomic complexity of MM, single-target drugs have limited efficacy and are prone to drug resistance. Therefore, there is an urgent need to develop multi-target drugs against MM. We screened drugs that simultaneously inhibit poly(ADP-ribose) polymerase 1 (PARP1) and 20S proteasome through computer-aided drug discovery (CADD) techniques, and explored the binding mode and dynamic stability of selected inhibitor to proteasome through Molecular biology (MD) simulation method. Thus, the dual-target inhibition effect of fluzoparib was proposed for the first time, and the ability of dual-target inhibition and tumor killing was explored at the enzyme, cell and animal level, respectively. This provides a theoretical and experimental basis for exploring multi-target inhibitory drugs for cancers.

1. Introduction

Multiple myeloma (MM) is a class of malignant plasma cell clonal proliferative diseases of the bone marrow. Approximately 10 % of all hematologic malignancies and 20 % of hematologic malignancies deaths [1]. Due to the high heterogeneity of tumor cells and the complex evolution of cloning, MM remains an incurable disease [2]. Therefore, there is an urgent need to develop multi-target drugs to overcome the heterogeneity and clonal evolution of MM cells.

Bortezomib, carfilzomib and ixazomib, which target the β-5 subunit of 20S proteasome, have been approved by the United States Food and Drug Administration for the treatment of multiple myeloma [3]. These drugs inhibit nuclear factor-kappa B (NF-κB) activation, promote the accumulation of misfolded and unfolded proteins, and inhibit the degradation of relevant receptor proteins in cells by competitively binding to the active sites of proteasomes, resulting in endoplasmic reticulum stress, which in turn plays a role in promoting apoptosis [4,5]. However, a single targeted drug may lead to tumor cell resistance, and the vast majority of patients relapse despite proteasome inhibitors [6]. More importantly, these drugs exhibit significant toxic side effects, for example, 30–60 % patients treated with bortezomib occur peripheral neuropathy [7] and Carfilzomib treatment is associated with cardiovascular toxicity [8] which restrict the clinical application. In a recent study, Velez et al. developed a series of potent and specific β2 inhibitor through using PI31's evolutionarily optimized inhibitory mechanisms, demonstrating that β2 can be a potential therapeutic target for multiple myeloma, which drove us to make more attempts to target the β2 subunit [9].

Poly(ADP-ribose) polymerase 1 (PARP1) is a cytoribozy present in eukaryotic cells that catalyzes polyADP-ribosylation, whose main role is to sense and recognize DNA single-stranded damage and initiate DNA damage repair pathway [10]. Studies have shown that inhibition of PARP1 can block the single-stranded DNA damage repair pathway of tumor cells, and eventually lead to the collapse of the cell system and apoptosis [11]. In MM, high expression of PARP1 was significantly associated with poor prognosis, which suggests that the PARP1 pathway may be a new option for improving treatment outcomes in MM patiens [12]. Proteasome inhibitors combined with PARP1 inhibitors promise to overcome cancer monotherapy resistance, enhance drug efficacy, and reduce single-drug dose toxicity. From the perspective of drug mechanism, inhibition of PARP1 and proteasome activity can aggravate intracellular stress from the genome level and protein level, respectively, and ultimately induce the collapse of the homeostatic system in tumor cells. Other results also confirm that bortezomib combined with the PARP1 inhibitor veliparib can synergistically exert an anti-MM effect [13]. However, there may be many drawbacks of drug combination, such as complex pharmacokinetic properties of each component,

* Corresponding author.
E-mail address: suyunwang2022@163.com (S. Wang).

https://doi.org/10.1016/j.bbrep.2024.101781
Received 28 February 2024; Received in revised form 5 June 2024; Accepted 5 July 2024

Abbreviations

MM	multiple myeloma
NF-κB	nuclear factor-kappa B
PARP1	poly(ADP-ribose) polymerase 1
CADD	computer-aided drug discovery
FBS	fetal bovine serum
PenStrep	penicillin-streptomycin
RIPA	radioimmunoprecipitation assay
CCK-8	cell counting kit-8
Annexin V-FITC/PI	fluorescein isothiocyanate-conjugated annexin V and propidium iodide
SPSS	stroke-physiological saline solution
DMSO	dimethyl sulfoxide
MD	molecular biology
PVDF	polyvinylidene fluoride
ANOVA	one-way analysis of variance
Alt-NHEJ	alternative non-homologous end joining

unpredictable biochemical reactions between metabolites, and increased drug toxicity [14,15]. Therefore, seeking suitable dual-target inhibitors that simultaneously inhibit proteasomes and PARP1 may be an ideal route for the treatment of refractory relapsed MM.

It is well known that de novo drug design is time-consuming and carries a great risk of failure [16]. In contrast, revealing a new clinical indications targeted for other signaling pathway from drugs with existing clinical trial appears to be an affordable and efficient drug development strategy [17–19]. Fluzopanib, as a PARP1 inhibitor, has been approved for the treatment of patients with platinum-sensitive recurrent ovarian, fallopian tube or primary peritoneal cancer. However, its dual-target inhibition potential remain unclear.

In our research, fluzoparib was first identified as a dual-target inhibitor through computer-aided drug discovery(CADD) techniques [20]. On the one hand, as for a kind of PARPi, fluzoparib capitalize on genomic instability caused by oxidative and replication stress, as well as deficiencies in DNA repair pathways. On the other hand, as for a kind of proteasome inhibitor, fluzoparib affect protein turnover. Notably, in our reserach, the anti-proteasome activity of fluzoparib is thought to occur by targeting on the β2 subunit of 20s proteasome. Revealing the synergistic effect of anti-dual targets of fluazopanib is expected to provide new ideas and basic research basis for the treatment of refractory relapsed MM.

2. Materials and methods

2.1. Materials

The human MM cell lines NCI–H929 (H929) and NCI–H929B (H929B, bortezomib-resistant) were sourced from Procell (Wuhan, Hubei, CHN). Fetal bovine serum (FBS), penicillin-streptomycin (PenStrep), RPMI-1640 medium, radioimmunoprecipitation assay (RIPA), and ECL Western Blotting Substrate were acquired from Thermo Fisher Scientific (Waltham, MA, USA). Bortezomib and fluzoparib were obtained from Jiangsu Hengrui Medicine Co. (Shanghai, CHN). Cell counting kit-8 (CCK-8) was sourced from Biosharp (Hefei, Anhui, CHN). Annexin V-FITC/PI apoptosis detection kit, TUNEL apoptosis assay kit, and cell cycle assay kit were purchased from BD Biosciences (Franklin Lakes, NJ, USA). Antibodies including BCL-2, BAX, FAS, P53, CCND1, *p*-ATM, ATM, cleaved-PARP, PARP, γH2AX, β-actin, and Ubiquitin were procured from Cell Signaling Technology (Danvers, MA, USA). Stroke-physiological saline solution (SPSS) and dimethyl sulfoxide (DMSO) were provided by Beyotime (Shanghai, CHN). BALB/c nude mice were obtained from Vital River Laboratories (Beijing, CHN). The 20S-PSM kit (SED321Hu 96T) was purchased from cloud-clone (Wuhan).

2.2. Dual-target inhibitory drug screening

Leveraging our previous foundational investigations, we identified 909 small molecule compounds exhibiting PARP1 inhibitory activity (IC50 $<$ 10 μM) sourced from the PubChem virtual chemical libraries as prospective proteasome inhibitor candidates. Specifically targeting the β2 active site of the 20S proteasome, denoted by PDB codes 6HTC, 6HTD, 6HTP, 6HTR, 6HUB, 6HUC, 6HUQ, 6HUU, 6HUV, 6HV4, 6HV5, 6HV7, 6HVA, 6HVR, 6HVS, 6HVT, 6HVU, 6HVV, and 6HVW, we conducted virtual screening experiments on 1548 small molecule compounds using the AutoDock Vina program and the web server MTiOpenScreen. Subsequently, the outcomes were scrutinized to assess compounds ripe for target repositioning. The evaluation and preliminary identification of candidate compounds with potential high affinity for proteasome active sites were based on the Gibbs free energy (ΔG) interactions between the compound and the corresponding target protein active site.

2.3. Cell culture

H929 and H929B cells were cultured in cell culture flasks containing growth medium composed of RPMI-1640 supplemented with 0.05 mM β-mercaptoethanol, 10 % FBS, and 1 % penicillin-streptomycin. The cells were maintained at 37 °C in a humidified 5 % CO2 atmosphere [21].

2.4. Cell viability assay

H929 and H929B cells were seeded at a density of 2×10^4 cells per well in 100 μL of their respective growth media in 96-well plates and incubated overnight for 18 h. The cells were then exposed to bortezomib concentrations ranging from 0.625 to 20 nM and fluzoparib concentrations ranging from 2.5 to 10 nM at 37 °C in a 5 % CO2 environment for 24 h. Subsequently, 10 μL of CCK-8 reagent was added to each well and incubated at 37 °C for 2 h. The absorbance at 450 nm was measured using a multi-plate reader (Varioskan LUX, Thermo Fisher Scientific). Cell viability at each concentration was determined as a percentage of the control, and the IC50 value was calculated with GraphPad Prism software [22].

2.5. Cell apoptosis and cycle assay

H929 and H929B cells were plated at a density of 4×10^5 cells per well in 2 mL of respective growth medium in 6-well plates overnight for 18 h. Cells were treated with 5 nM bortezomib and increasing concentrations of fluzoparib (2.5, 5, and 10 nM) at 37 °C and 5 % CO_2 for 24 h. After the completion of the time point, cells were washed three times by 1 × PBS. Cells were treated with Annexin V-FITC/PI for apoptosis analysis [23]. Cells were fixed in 70 % ice ethanol overnight and then stained with PI/RNase staining buffer for cycle analysis [24]. The percentage of cells undergoing apoptosis or cycle in each treatment cohort was analyzed by flow cytometry (Gallios, Beckman Coulter).

2.6. Western blot

Western blot analysis was conducted to assess intracellular and intratumor protein levels. Tumor tissues weighing 100 mg were extracted from the sacrificed nude mice by neck removal. Protein extraction was performed using RIPA lysis buffer supplemented with 1 × protease inhibitor cocktail (PMSF) for both cell and tumor tissue samples. The crude lysates were clarified using an ultrasonic cell pulverizer and centrifuged at 12,000 rpm for 15 min at 4 °C. Subsequently, 50 μg of total proteins were separated on 12 % gradient gels (Bio-Rad) and transferred onto polyvinylidene fluoride (PVDF) membranes. The

membranes were then incubated overnight at 4 °C with primary antibodies including β-actin, BCL-2, BAX, FAS, P53, CCND1, Ubiquitin, *p*-ATM, ATM, PARP, Cleaved-PARP, γH2AX, H2AX, ATM, and *p*-ATM (all used at a dilution of 1:1000). Following primary antibody incubation, the blots were probed with horseradish peroxidase-conjugated goat anti-rabbit IgG (H + L) secondary antibody and visualized using ECL Western Blotting Substrate with a ChemiDoc MP imager [25,26] (Bio-Rad). Image Pro Plus 6.0 software was utilized to analyze and report the normalized band intensity for quantifying relative protein expression levels.

2.7. Animal models

All animal studies were conducted in compliance with the approved ethics protocol by the Institutional Animal Care and Use Committee at the Institute of Biophysics, Chinese Academy of Sciences. Female BALB/c nude mice aged 5–7 weeks were housed in a specific pathogen-free (SPF) barrier system under controlled conditions of constant temperature (26–28 °C) and humidity (40%–60 %), and provided with sterile food and water. H929B cells were prepared at a concentration of 2×10^6 cells suspended in a PBS and matrigel solution (PBS:matrigel = 1:1), and 200 μL of the cell suspension was subcutaneously injected into the armpit of nude mice [27]. Upon reaching a tumor volume of 100 mm^3, the mice were randomly assigned into control and experimental groups: the fluzoparib group (30 mg/kg) and the bortezomib group (1 mg/kg), each consisting of seven mice. Fluzoparib was dissolved in a solution of 10 % DMSO and 90 % SPSS for oral administration at a daily dose of 200 μL per mouse. Bortezomib was dissolved in 100 % SPSS and administered intravenously twice a week with a dosage of 200 μL per mouse. Tumor size was monitored every other day using calipers until the endpoint, defined as when the longest tumor diameter reached 13–15 mm or tumors showed signs of ulceration. Tumor volume was calculated using the formula: $V = 0.5 \times a \times b2$ (where a represents the longest diameter and b the shortest diameter). Prior to tissue and organ collection, the nude mice were humanely euthanized by neck removal. Tumor apoptosis was assessed using the TUNEL assay following fixation with 4 % paraformaldehyde. In the in vivo proteasome activity assay, tumor cells were isolated from the tissue and digested with pancreatic enzymes, then plated in 96-well plates at a concentration of 3×10^5 cells per well. Drugs were added according to the experimental groups, followed by incubation. An equal volume of the proteasome assay solution was added, and the plates were then incubated at 37 °C or room temperature for at least 1 h. Fluorescence intensity was measured at Ex/Em = 490/525 nm using a fluorescent zymograph.

2.8. Proteasome activity assay

The proteasome activity of tumor cells cultured in 2.7 was evaluated using ELISA [28] and the Proteasome 20S Activity Assay Kit [29]. In the ELISA procedure, reagents, samples, and standards were initially prepared. Subsequently, 100 μL of standard or sample was added to each well, followed by a 1-h incubation at 37 °C. The solution was then aspirated, and 100 μL of prepared Detection Reagent A was added, followed by another 1-h incubation at 37 °C. After aspiration, the wells were washed three times, and 100 μL of prepared Detection Reagent B was added, followed by a further 30-min incubation at 37 °C. The solution was then aspirated, washed five times, and 90 μL of Substrate Solution was added. Following an incubation period of 10–20 min at 37 °C, 50 μL of Stop Solution was added, and the absorbance was immediately measured at 450 nm. In the Proteasome 20S Activity Assay Kit (Fluorometric) section, cells were treated with test compounds (100 μL per well in a 96-well plate), and an equal volume of proteasome assay solution (100 μL per well in a 96-well plate) was added. The mixture was incubated at 37 °C or room temperature for at least 1 h, with fluorescence intensity monitored at Ex/Em = 490/525 nm.

2.9. Statistical analyses

All results were expressed as means ± SEM, unless otherwise shown. P value was determined using unpaired, two-tailed Student's t tests and one-way analysis of variance (ANOVA) with Tukey's post hoc test; the criterion for statistical significance was taken as $P < 0.05$.

3. Results

3.1. Fluzoparib as a potential dual-target inhibitory drug

The results of virtual scoring and cross-validation of the top 100 compounds are shown in Fig. 1A. The overall score distribution of 909 compounds were 2.0–10.0, while the first 100 compounds was 8.1–10.0, which showed spontaneous affinity for the proteasome active sites and basically had the molecular structure basis of proteasome inhibitors. The list of proteasome inhibition candidate compounds we screened we uploaded as a supplementary file(Supplementary file 1). Structural similarity clustering analysis was performed on selected 100 compounds by the hierarchical clustering function of ChemBioServer 2.0 [30]. Among them, 39 compounds can be clustered into 3 subsets (Cluster 1, Cluster 2, Cluster 3) with similar parent structures, and the general formula of the parent structure is shown in Fig. 1B. Fluzoparib (PubChem CID: 56649297) is a representative compound in Cluster 1. Furthermore, the compounds with higher scores are BDBM50427935 (PubChem CID: 71605392), CHEMBL3902201 (PubChem CID: 73052006), BDBM50427927 (PubChem CID: 71604717). The structure of Bortezomib (PubChem CID: 3874471) was also uploaded as a positive control(Fig. 1C). The results of Fluzoparib docking with the active site of the proteasome are shown (Fig. 1D). From this, we speculated that fluzoparib and other higher-scoring compounds may have proteasome and PARP1 dual-target inhibition activity.

3.2. Fluzoparib treatment reduces the viability and induces apoptosis of MM cells

To explore the effect of fluzoparib on the viability of MM cells, cells were treated with different concentrations of fluzoparib or bortezomib. CCK-8 solution was used to assess cell viability. The positive control drug bortezomib only significantly inhibited the proliferation of H929 cells (IC_{50} values = 5.6 nM, Fig. S1A), but had no obvious effect on bortezomib-resistant H929B cells (Fig. 2A). In contrast, a significant reduction was observed in the cell viability of H929 and H929B cells in a fluzoparib concentration-dependent manner (Fig. 2B). IC50 for H929 and H929B cells was observed at 11.88 nM and 12.40 nM (Figs. S1B and C). Similarly, Olaparib inhibited the survival of H929 and H929B cells in a concentration-dependent manner(Fig. 2C) and IC50 for H929 and H929B cells was observed at 25.76 μM and 34.43 μM (Figs. S1D and E).

The fluzoparib-mediated reduction in cell viability prompted us to evaluate if the MM cells undergo apoptosis upon exposure to fluzoparib. Therefore, Annexin V-FITC/PI dual staining experiment was performed using flow cytometry. The quadrants represent the viable cell population (lower-left quadrant), early apoptotic cell population (lower-right quadrant), late apoptotic cell population (upper-right quadrant) and necrotic cell population (upper-left quadrant), respectively [31]. A concentration-dependent increase in apoptosis was observed upon treatment of H929 cells with increasing concentrations of fluzoparib (2.5 nM, 5.0 nM, and 10 nM), and 10 nM fluzoparib significantly promoted apoptosis in H929 and H929B cells. However, bortezomib only promoted apoptosis of H929 cells, but the effect on bortezomib-resistant H292B cells was not obvious (Fig. 2D and Fig. S2A). These results indicate that fluzoparib efficiently induces apoptotic cell death in H929 and H929B cells.

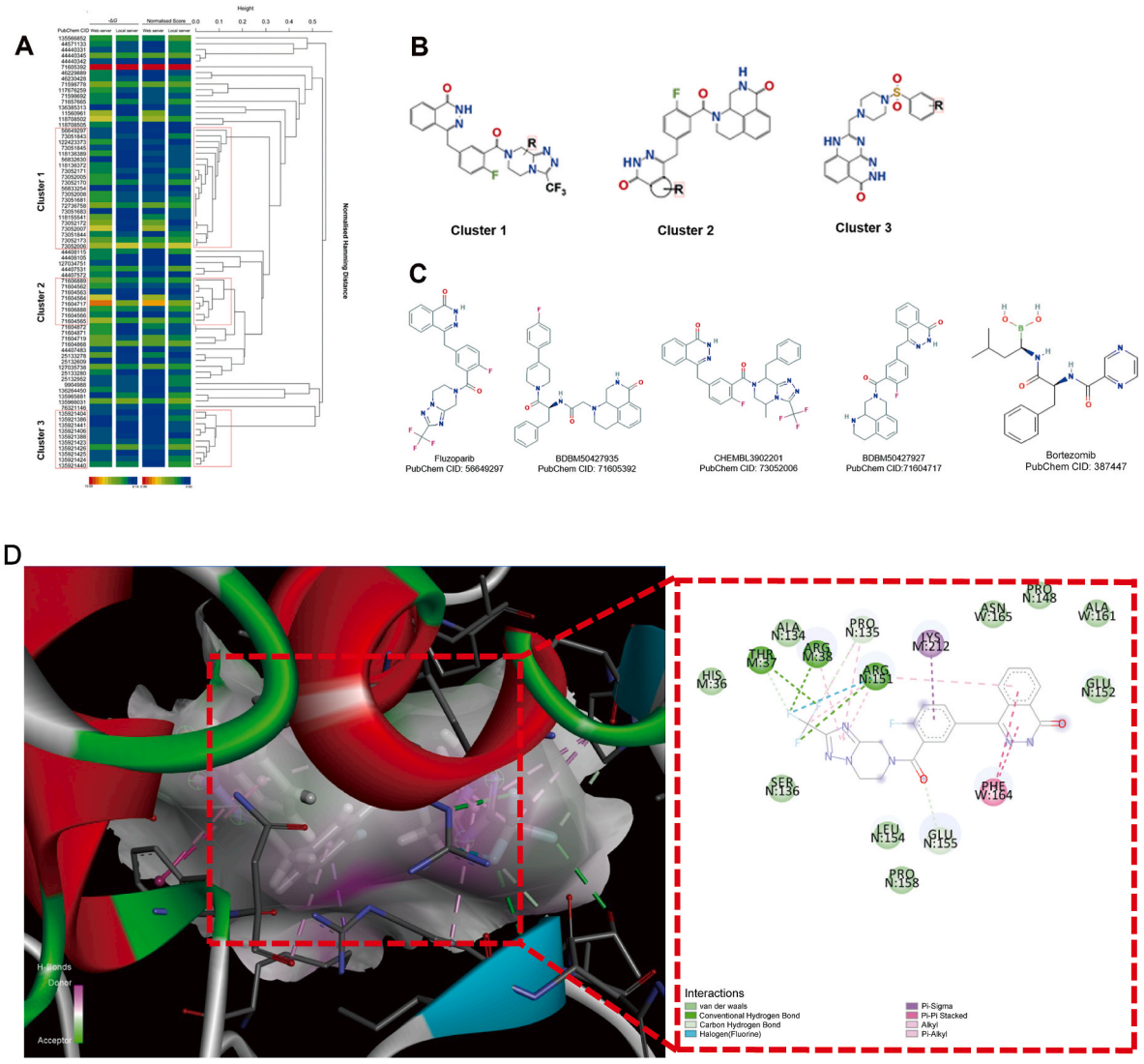

Fig. 1. CADD techniques screening for dual-target inhibitors. (A) Heat map of scoring results and structural cluster analysis for 100 candidate compounds. "Web server" stand for MTiOpenScreen online service filtering; "local server" mean AutoDock Vina software for local data filtering; "-ΔG" indicates that the affinity and Gibbs free energy reaches a negative value; "normalized score" indicates the scoring result after normalizing the min-max normalization data by filtering the scoring value. The low to high scoring values are indicated by blue-green-red blocks. The compounds in the red box are clustered into compounds in the same subset based on structural similarity. (B) Structural similarity cluster analysis revealed the parent structure of 3 clustered compounds. (C) The structure of the 5 highest-scoring and common inhibitors such as fluzoparib. (D) The receptor-ligand interactions of fluzoparib with proteasome. (For interpretation of the references to colour in this figure legend, the reader is referred to the Web version of this article.)

3.3. Fluzoparib arrests MM cells cycle

During the cell cycle from G_2 phase to mitotic period, DNA damage checkpoints need to be passed to confirm the integrity and correctness of the cell genome, and if the delay of DNA checkpoints increases due to the extension of the cell G_2 phase, the cell will initiate the apoptosis process [32]. As shown in Fig. 2E, both fluzoparib and bortezomib were able to arrest the H929 cell cycle in the G_2/M phase. However, acting on H929B cells, fluzoparib arrested cells in the G_2/M phase at 26.3 % (2.5 nM), 44.9 % (5 nM), and 69.5 % (10 nM), which was significantly higher than the rate of blockade of 5 nM bortezomib (11.7 %) (Fig. S2B). The experimental results show that fluzoparib causes apoptosis by arresting the cycle of MM cells in the G_2/M phase, and also as effective against bortezomib-resistant MM cell line.

3.4. Fluzoparib promotes tumor cell apoptosis by acting on PARP and proteasome degradation pathway

To figure out the detailed mechanism of action of Fluzoparib, we first examined changes in protein levels related to proteasome inhibitor and PARP axis-related pathway. Indeed, proteasome inhibitors and PARP inhibitors inhibit tumor growth by acting on the cell cycle, apoptosis and DNA damage repair pathways, respectively [5,33,34]. Western blot assay revealed that fluzoparib downregulated the anti-apoptotic protein BCL-2, cell cycle-related protein CCND1 in H929 cells and its bortezomib-resistant cells, which suggested that fluzoparib can affect the proteasome pathway (Fig. 3A). Notably, 20S proteasome activity level was significantly down-regulated after treated with Fluzoparib and Bortezomib in H929 cell(Fig. 3B–C). Bortezimib, a classical proteasome inhibitor used as a positive control, exerted these effects only in H929 cells and was ineffective in H929B-resistant cells(Figs. S3A–B). However, the effect of Fluzoparib in H929B-resistant cells was still significant, suggesting that Fluzoparib may also exert its anti-tumor effects

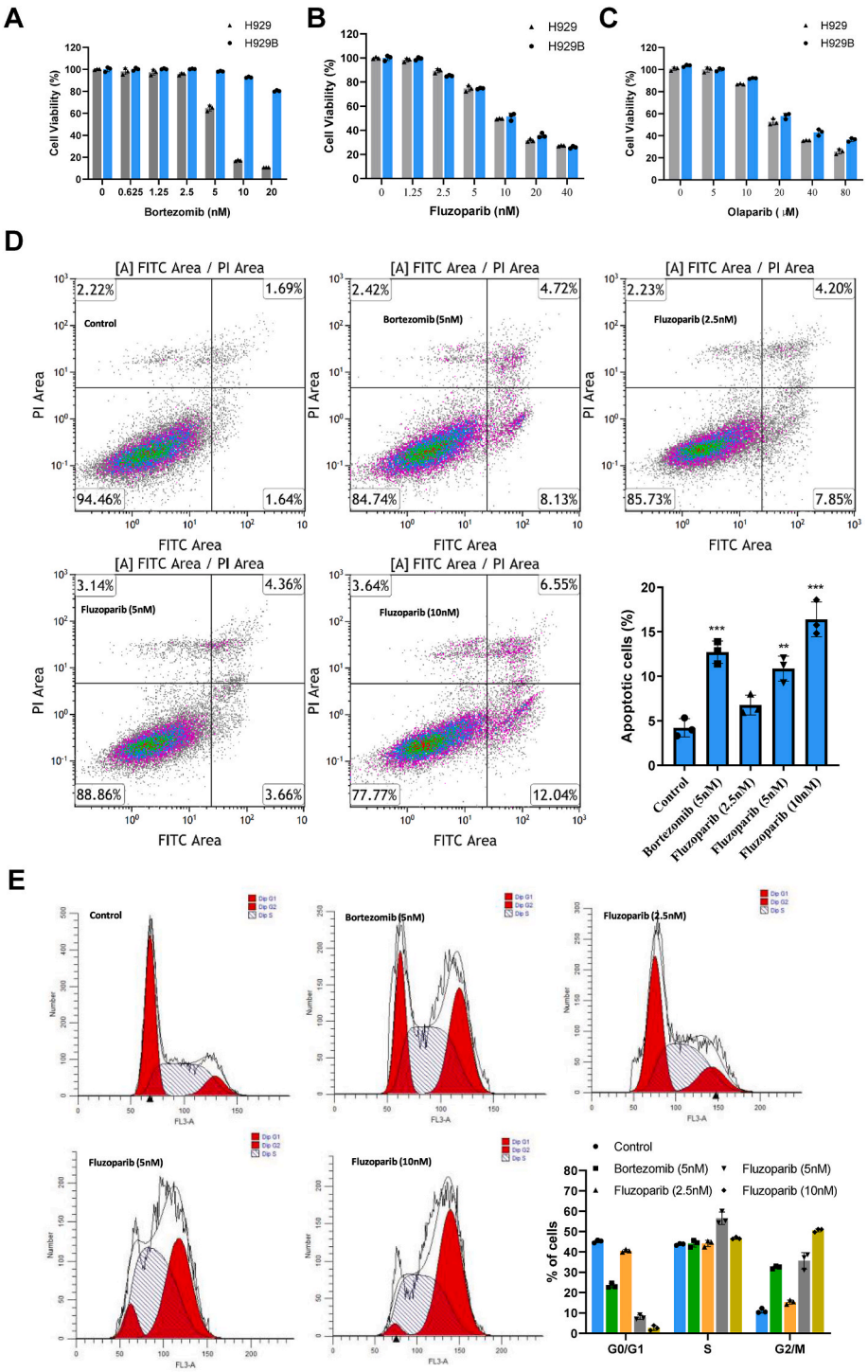

Fig. 2. Activity effects of fluzoparib on H929 and H929B cells. (A, B, C) CCK8 assay after treatment of H929, H929B cells with different concentrations of drugs (Bortezomib:0, 0.625, 2, 5, 5, 10, 20 nM; Fluzoparib:0, 1.25, 2.5, 5, 10, 20, 40 nM; Olaparib:0, 5, 10, 20, 40, 80 μM). Data are presented as the mean ± SD. Bortezomib inhibited significantly inhibited the proliferation of H929 cells but had no effect on H929B cells.Fluzoparib with Olaparib significantly inhibited the proliferation of H929 and H929B cells. (A). Bortezomib. (B). Fluzoparib. (C). Olaparib. (D). Apoptosis assays after treatment of H929 cell with different concentrations of drugs:Control, Bortezomib(5 nM) and Fluzoparib(2.5, 5, 10 nM), detected by flow cytometry. Both Bortezomib and Fluzoparib Significantly Promote Apoptosis in H929 Cells. (E) and arrested cell cycle of H929. ***P < 0.001, **P < 0.01. n = 3. Fluzoparib and bortezomib were able to arrest the H929 cell cycle in the G2/M phase.

through other pathways, such as the PARP pathway. On the other hand, we examined the altered levels of PARP pathway-related proteins after treated with Bortezomib, Olaparib(Classical PARPi, which serve as a positive control) and Fluzoparib. Western blot assay revealed that both Olaparib and Fluzoparib significantly up-regulated cleaved-PARP and DNA damage repair-related γH2AX protein levels. (Fig. 3D, Fig. S3D), which indicated that Fluzoparib can affect PARP pathway.

The precise regulatory mechanism in the cell enables the degradation and modification of endogenous proteins to be carried out in an orderly manner, ensuring the homeostasis of the internal environment and the

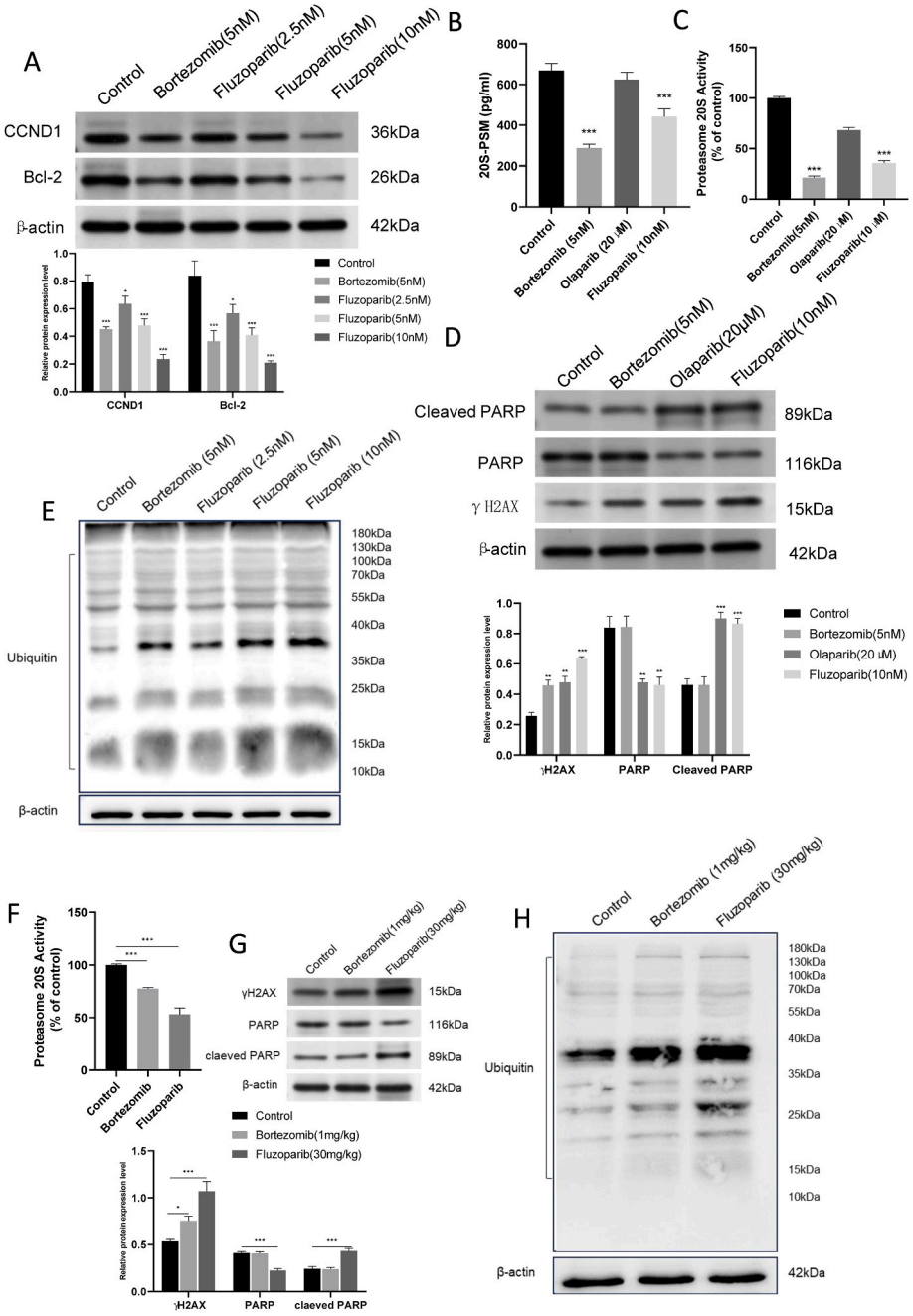

Fig. 3. Fluzoparib inhibits the protein degradation function of proteasome, allowing the accumulation of ubiquitinated proteins and/or mis-folded can proteins leading to apoptosis. (A-E)In vitro assay. (A). Western blotting assay after treated with Bortezomib(5 nM) and Fluzopanib(2.5, 5 and 10 nM). Both Bortezomib and Fluzoparib down-regulated cell cycle-related proten CCND1 and pro-apoptotic protein Bcl-2 in H929 cell. (B). 20S-PSM assay was conducted through Proteasome 20S Activity Assay Kit. H929 cell was treated with Control, Bortezomib, Olaparib and Fluzopanib. Both Bortezomib and Fluzopanib can significantly down-regulated 20s-PSM level. n = 3 per group. vs Control, *P < 0.05; **P < 0.01; ***P < 0.001. (C). Proteasome 20S activity assay was conducted through Proteasome 20S Activity Assay Kit (Fluorometric). H929 cell was treated with Control, Bortezomib, Olaparib and Fluzopanib. Both Bortezomib and Fluzopanib can significantly down-regulated proteasome 20s-PSM activity. (D). Western blotting assay after treated with Bortezomib(5 nM), Olaparib(20 μM) and Fluzopanib(10 nM). Both Olaparib and Fluzoparib can up-regulated Cleaved-PARP and γH2AX protein level in H929 cell. (E). Compared with control and Bortezomib group, H929 treated with Fluzoparib can enhance endogenous polyubiquitination level. (F–H) In vivo assay. (F) Fluzopanib can significantly up-regulated proteasome 20s-PSM activity. (G). Western blotting assay after treated with Bortezomib(1 mg/kg) and Fluzopanib(30 mg/kg). Fluzoparib can up-regulated Cleaved-PARP and γH2AX protein level. (H). Compared with control and Bortezomib group, treated with Fluzoparib can enhance endogenous polyubiquitination level.

orderly progress of physiological activities. Among them, the ubiquitin-proteasome degradation pathway in eukaryotes regulates many normal cellular processes [35]. In previous studies, we have confirmed the growth inhibition, apoptosis induction and cycle arrest effects of fluzoparib on MM cells, so we investigated whether the mechanism is related to changes in the ubiquitination of endogenous proteins in cells. The results of Fig. 3E and Fig. S3E showed that fluzoparib enhanced the level of endogenous protein polyubiquitination in H929 cells as bortezomib, and was equally effective against bortezomib-resistant MM cells. The results show that fluzoparib inhibits the protein degradation function of proteasome, allowing the accumulation of ubiquitinated proteins and/or mis-folded can proteins leading to apoptosis. The above results

we arrive at the same trend in vivo(Fig. 3F–H). In vivo experiments, the use of bortezomib and fluzoparib reduced the activity of the proteasome by about 20 % and 45 %, respectively. The level of ubiquitination also increased after treatment. These are consistent with the results in vivo and in vitro.

3.5. Fluzoparib forestalls the outgrowth of tumor in vivo

We further explored the treatment affect of fluzoparib in subcutaneous murine MM tumor models in vivo. Start with the treatment of tumor-bearing mice, measured tumor volumes with calipers every two days. The tumor size in the fluzoparib-treated group was significantly less than in the untreated group and bortezomib-treated group from day 1 through day 13 (Fig. 4A). Compared with bortezomib, fluzoparib significantly suppressed tumor volumes (Fig. 4B) and weights (Fig. 4C). The concentrations of fluzoparib administered were well tolerated by mice, without significant weight loss (Fig. 4D). To detect apoptotic cells in the xenograft tumors excised from mice, lesions from the three groups of mice were stained by the TUNEL method. Typically, the TUNEL stain was punctate, but in some cases the TUNEL signal was more diffuse and presumably representing relatively early-versus late-stage apoptosis, respectively [36]. As expected, TUNEL-positive cells were much frequent in fluzoparib-treated mice than control and bortezomib-treated mice, representing more significant apoptosis (Fig. 4E and F). These data demonstrate the potent antitumor activity of fluzoparib in vivo. Importantly, these findings also show that fluzoparib is orally bioactive and provides a preclinical framework for its evaluation as an oral agent in phase I trials in MM.

4. Discussion

The primary objective in treating patients with MM is to improve both survival duration and quality of life by managing disease-related complications through long-term suppression of the cancer. Notable progress has been made recently with the advent of proteasome inhibitors such as bortezomib, immunomodulatory drugs like thalidomide, monoclonal antibodies that target myeloma cell surface antigens such as daratumumab, and autologous hematopoietic stem cell transplantation [37–40]. While a small subset of patients may achieve a cure or sustained remission after initial treatment, the majority will eventually experience disease recurrence leading to mortality [41]. Thus, MM remains an untreatable condition, underscoring the need for the development of multitarget drugs to combat the variety and evolutionary changes seen in the disease [42,43]. An example of such a drug is Fluzoparib, a new, potent PARP1/2 inhibitor that can be taken orally and has shown significant anticancer effects [44–46] with minimal added toxicities [47]. It has gained approval for treating ovarian cancer, and ongoing phase II and III trials are exploring its efficacy in treating various solid tumors, including those affecting the pancreas, breast, prostate, and lungs [48]. Nevertheless, the role of Fluzoparib in multiple myeloma remains ambiguous. In our research, Fluzoparib was identified as a type of proteasome inhibitor using computer-aided drug design

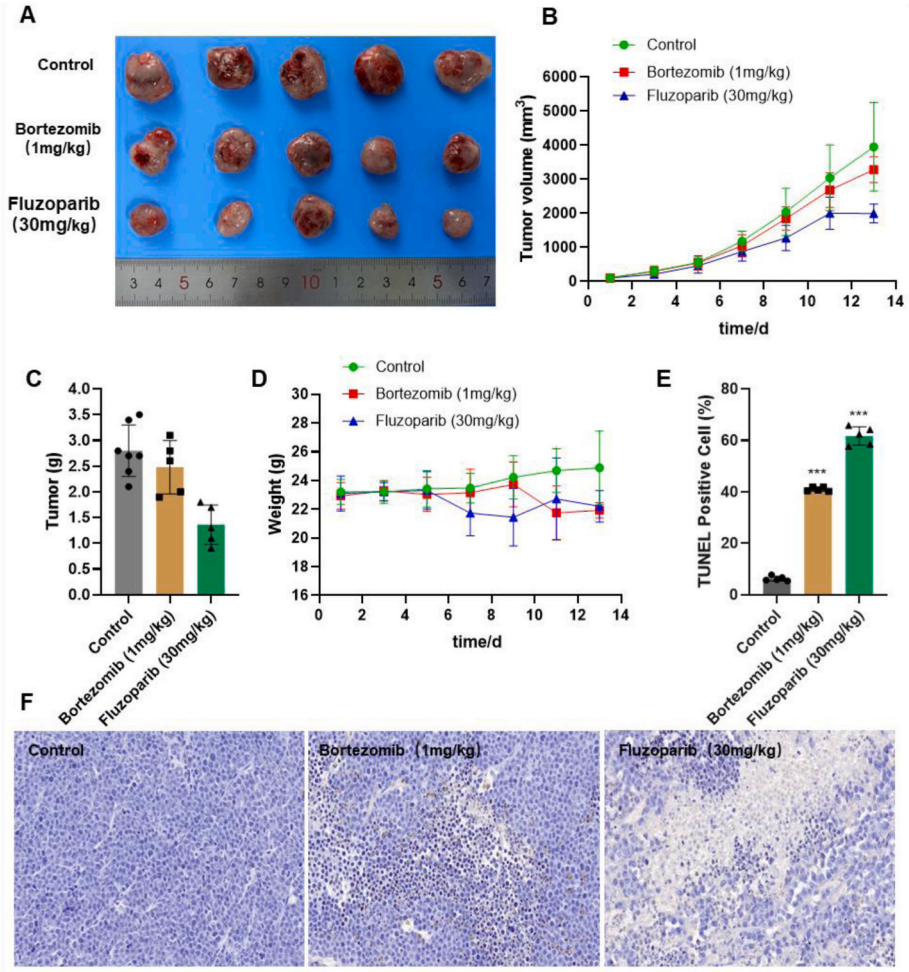

Fig. 4. Fluzoparib suppressed tumor growth of MM in vivo. (A) Representative images are presented illustrating the difference between the groups in tumor size after drug treated two weeks. Fluzoparib reduced tumor volumes (B) and weights (C) of nude mice. (D) Fluzoparib had less effect on body weight in nude mice. (E, F) TUNEL staining showed that fluzoparib promoted apoptosis of tumor tissue. ***$P < 0.001$. $n = 3$.

techniques. Does Fluzoparib's antitumor activity also involve proteasome inhibition? Therefore, in our current investigation, we aimed to assess Fluzoparib's potential to deliver anticancer effects through the PARP1 and proteasome pathways in multiple myeloma cells. Our results indicate that Fluzoparib exhibits robust anti-multiple myeloma activity in both in vitro and in vivo settings and boasts a favorable toxicity profile, primarily attributable to two classical mechanisms, as discussed below.

Firstly, Fluzoparib demonstrates potent proteasome inhibition in vivo. Proteasomes, a distinct type of proteolytic enzyme, are distributed in the nucleus and cytoplasm of all cells, constituting up to 1 % of the total cell protein [49,50]. Cellular protein homeostasis relies on the proteasome [51–53]. Malignant cells rely more heavily on the proteasome to eliminate misfolded or damaged proteins due to their genetic instability and rapid proliferation [54]. Fluzoparib's mechanism of proteasome inhibition mirrors that of bortezomib—they both directly bind to and inhibit the enzyme complex, leading to the accumulation of ubiquitinated proteins and eventual apoptosis. Notably, Fluzoparib downregulates the expression of the anti-apoptotic protein BCL-2 and cell cycle-associated protein CCND1 to a greater extent compared to bortezomib (Fig. 3A). While proteasome inhibition stands as a pivotal therapeutic approach for multiple myeloma, nearly all patients eventually develop resistance to proteasome inhibitors [55]. Moreover, the considerable toxic side effects associated with these drugs pose limitations on the long-term efficacy of treating multiple myeloma through the proteasome pathway [7]. Interestingly, Fluzoparib demonstrated substantial tumor cell eradication even in proteasome-resistant cells, representing a noteworthy aspect.

Secondly, Fluzoparib exhibits significant inhibition of PARP1 in vivo. PARP1, a pivotal member of the poly(ADP-ribose) polymerases family, plays a crucial role as a binding platform for various other proteins and governs a multitude of cellular processes, including but not limited to DNA repair, transcription, cell death, chromatin remodeling, inflammation, metabolic regulation, cell cycle control, differentiation, proteasomal degradation, RNA processing, and modulation of tumor suppressors [56,57]. These discoveries have propelled PARP1 into the spotlight as a promising target for chemotherapy [58]. Fluzoparib demonstrates strong inhibitory effects on the PARP1 enzyme, resulting in evident G2/M phase arrest, apoptosis, and targeted eradication of MM cells, along with a dose-dependent anti-proliferative impact on bortezomib-resistant MM cells.

In essence, the mechanism of action of Fluzoparib in treating MM is elucidated in Fig. 5. On one front, Fluzoparib suppresses PARP1 activity, impeding the repair of damaged DNA and directing it towards the alternative non-homologous end-joining (Alt-NHEJ) pathway [11], leading to the production of faulty proteins. Simultaneously, Fluzoparib's inhibition of proteasome activity prevents the timely degradation of these faulty proteins. The combined effect of both actions disrupts cellular homeostasis, ultimately culminating in apoptosis. Notably, the bioavailability of Fluzoparib in female nude mice surpasses that of bortezomib. These characteristics collectively position Fluzoparib as a drug with favorable pharmacodynamic properties, lending support to its progression through clinical trials.

5. Statement

All experiments and methods were performed in accordance with the ARRIVE guidelines and regulations. All methods were carried out in accordance with relevant guidelines and regulations.

Funding

This work was supported by Shenzhen Science and Technology Program (No. JCYJ20210324141007017 and No. JCYJ20230807151307015) and Shenzhen Longhua District Foundation of Science and Technology (No.11501A20220923BF690D7).

Ethical declarations

All experimental procedures were approved by Animal Ethics

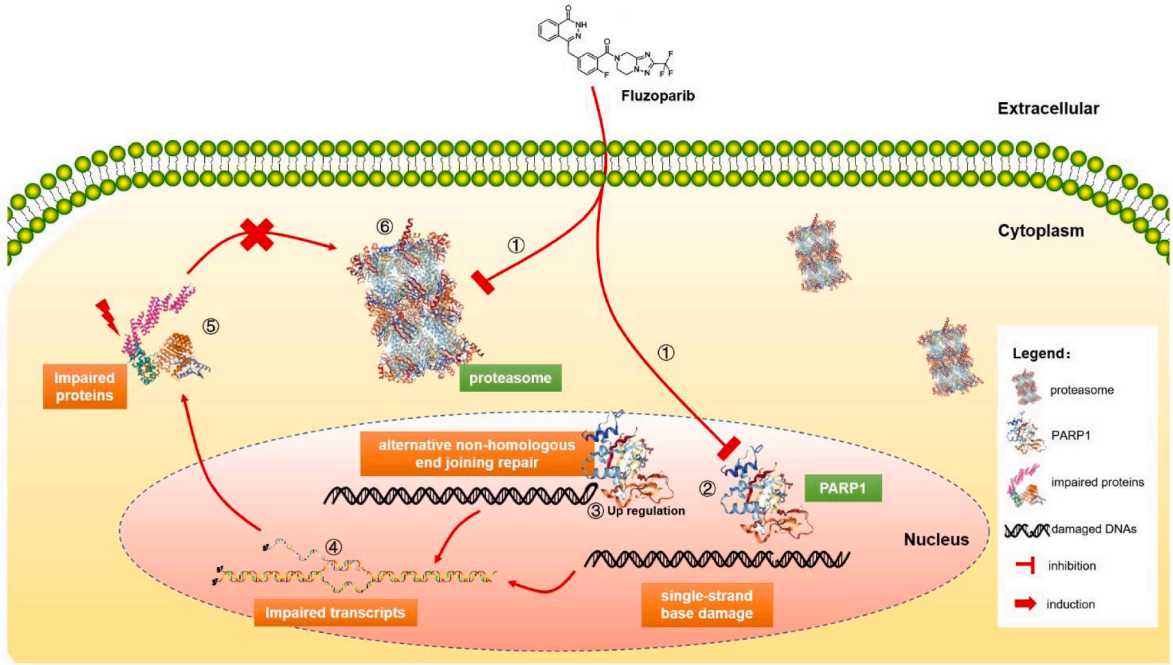

Fig. 5. Schematic diagram of the mechanism of action of fluzoparib as a dual-target inhibitory drug against MM cells. ①Fluzoparib inhibits the activity of proteasome and PARP1, respectively. ②Inhibition of PARP1 leads to DNA damage that cannot be repaired. ③The damaged DNAs are eventually repaired by the Alt-NHEJ pathway, during which PAPR1 is highly expressed and is a marker of drug resistance in various tumors. ④Damaged DNAs are transcribed into impaired transcripts. ⑤Partially impaired transcripts are translated into impaired proteins. ⑥Proteasomes activity are inhibited, and impaired proteins cannot be degraded in time.

Committee of Guangdong Medical University (GDY2302374).

CRediT authorship contribution statement

Kai Deng: Investigation, Formal analysis, Data curation. **Qiongqiong Li:** Validation, Supervision, Software. **Lina Lu:** Writing – review & editing, Writing – original draft, Visualization, Validation. **Luting Wang:** Supervision, Software, Resources, Project administration. **Zhiyong Cheng:** Resources, Project administration, Methodology, Investigation, Funding acquisition. **Suyun Wang:** Data curation, Conceptualization.

Declaration of competing interest

The authors declare no potential conflicts of interest.

Data availability

Data will be made available on request.

Acknowledgements

The authors thank all members of the Department of Orthopedics, Department of Hematology, Shenzhen Longhua District Central Hospital and Department of Hematology, Baoding No.1 Hospital for helpful comments and suggestions.

Appendix A. Supplementary data

Supplementary data to this article can be found online at https://doi.org/10.1016/j.bbrep.2024.101781.

References

[1] C. Wenzinger, E. Williams, A.A. Gru, Updates in the pathology of precursor lymphoid neoplasms in the revised fourth edition of the WHO classification of tumors of hematopoietic and lymphoid tissues, Curr Hematol Malig Rep 13 (2018) 275–288, https://doi.org/10.1007/s11899-018-0456-8.
[2] R.A. Kyle, et al., Long-term follow-up of monoclonal gammopathy of undetermined significance, N. Engl. J. Med. 378 (2018) 241–249, https://doi.org/10.1056/NEJMoa1709974.
[3] S. Gandolfi, et al., The proteasome and proteasome inhibitors in multiple myeloma, Cancer Metastasis Rev. 36 (2017) 561–584, https://doi.org/10.1007/s10555-017-9707-8.
[4] S.V. Rajkumar, P.G. Richardson, T. Hideshima, K.C. Anderson, Proteasome inhibition as a novel therapeutic target in human cancer, J. Clin. Oncol. 23 (2005) 630–639, https://doi.org/10.1200/JCO.2005.11.030.
[5] E.E. Manasanch, R.Z. Orlowski, Proteasome inhibitors in cancer therapy, Nat. Rev. Clin. Oncol. 14 (2017) 417–433, https://doi.org/10.1038/nrclinonc.2016.206.
[6] G.P. Soriano, et al., Proteasome inhibitor-adapted myeloma cells are largely independent from proteasome activity and show complex proteomic changes, in particular in redox and energy metabolism, Leukemia 30 (2016) 2198–2207, https://doi.org/10.1038/leu.2016.102.
[7] T.A. Thibaudeau, D.M. Smith, A practical review of proteasome pharmacology, Pharmacol. Rev. 71 (2019) 170–197, https://doi.org/10.1124/pr.117.015370.
[8] J.E. Park, Z. Miller, Y. Jun, W. Lee, K.B. Kim, Next-generation proteasome inhibitors for cancer therapy, Transl. Res. 198 (2018) 1–16, https://doi.org/10.1016/j.trsl.2018.03.002.
[9] B. Velez, et al., Rational design of proteasome inhibitors based on the structure of the endogenous inhibitor PI31/Fub1, Proc Natl Acad Sci U S A 120 (2023) e2308417120, https://doi.org/10.1073/pnas.2308417120.
[10] A. Ray Chaudhuri, A. Nussenzweig, The multifaceted roles of PARP1 in DNA repair and chromatin remodelling, Nat. Rev. Mol. Cell Biol. 18 (2017) 610–621, https://doi.org/10.1038/nrm.2017.53.
[11] M. Rouleau, A. Patel, M.J. Hendzel, S.H. Kaufmann, G.G. Poirier, PARP inhibition: PARP1 and beyond, Nat. Rev. Cancer 10 (2010) 293–301, https://doi.org/10.1038/nrc2812.
[12] P. Neri, et al., Bortezomib-induced "BRCAness" sensitizes multiple myeloma cells to PARP inhibitors, Blood 118 (2011) 6368–6379, https://doi.org/10.1182/blood-2011-06-363911.
[13] J. Blade, et al., Extramedullary disease in multiple myeloma: a systematic literature review, Blood Cancer J. 12 (2022) 45, https://doi.org/10.1038/s41408-022-00643-3.
[14] D. Godeau, A. Petit, I. Richard, Y. Roquelaure, A. Descatha, Return-to-work, disabilities and occupational health in the age of COVID-19, Scand. J. Work. Environ. Health 47 (2021) 408–409, https://doi.org/10.5271/sjweh.3960.
[15] D.S. Bell, Combine and conquer: advantages and disadvantages of fixed-dose combination therapy, Diabetes Obes Metab 15 (2013) 291–300, https://doi.org/10.1111/dom.12015.
[16] K. Park, A review of computational drug repurposing, Transl Clin Pharmacol 27 (2019) 59–63, https://doi.org/10.12793/tcp.2019.27.2.59.
[17] J. Dinic, et al., Repurposing old drugs to fight multidrug resistant cancers, Drug Resist Updat 52 (2020) 100713, https://doi.org/10.1016/j.drup.2020.100713.
[18] Y. Zheng, et al., Old drug repositioning and new drug discovery through similarity learning from drug-target joint feature spaces, BMC Bioinf. 20 (2019) 605, https://doi.org/10.1186/s12859-019-3238-y.
[19] K.A. O'Connor, B.L. Roth, Finding new tricks for old drugs: an efficient route for public-sector drug discovery, Nat. Rev. Drug Discov. 4 (2005) 1005–1014, https://doi.org/10.1038/nrd1900.
[20] S.J. Macalino, V. Gosu, S. Hong, S. Choi, Role of computer-aided drug design in modern drug discovery, Arch Pharm. Res. (Seoul) 38 (2015) 1686–1701, https://doi.org/10.1007/s12272-015-0640-5.
[21] R.P. Dutta, et al., Targeting transcriptional kinase of CDK7 halts proliferation of multiple myeloma cells by modulating the function of canonical NF-kB pathway and cell cycle regulatory proteins, Transl Oncol 35 (2023) 101729, https://doi.org/10.1016/j.tranon.2023.101729.
[22] D. Zhang, et al., Transcriptomic characterization revealed that METTL7A inhibits melanoma progression via the p53 signaling pathway and immunomodulatory pathway, PeerJ 11 (2023) e15799, https://doi.org/10.7717/peerj.15799.
[23] A. Rafat, et al., Telomerase inhibition on acute myeloid leukemia stem cell induced apoptosis with both intrinsic and extrinsic pathways, Life Sci. 295 (2022) 120402, https://doi.org/10.1016/j.lfs.2022.120402.
[24] C. Lang, et al., m(6) A modification of lncRNA PCAT6 promotes bone metastasis in prostate cancer through IGF2BP2-mediated IGF1R mRNA stabilization, Clin. Transl. Med. 11 (2021) e426, https://doi.org/10.1002/ctm2.426.
[25] Y. Bagheri, et al., Comparative study of gavage and intraperitoneal administration of gamma-oryzanol in alleviation/attenuation in a rat animal model of renal ischemia/reperfusion-induced injury, Iran J Basic Med Sci 24 (2021) 175–183, https://doi.org/10.22038/IJBMS.2020.51276.11642.
[26] E. Fathi, S.A. Mesbah-Namin, I. Vietor, R. Farahzadi, Mesenchymal stem cells cause induction of granulocyte differentiation of rat bone marrow C-kit(+) hematopoietic stem cells through JAK3/STAT3, ERK, and PI3K signaling pathways, Iran J Basic Med Sci 25 (2022) 1222–1227, https://doi.org/10.22038/IJBMS.2022.66737.14633.
[27] L.D. Ma, et al., Morinda citrifolia (noni) juice suppresses A549 human lung cancer cells via inhibiting AKT/nuclear factor-kappa B signaling pathway, Chin. J. Integr. Med. 27 (2021) 688–695, https://doi.org/10.1007/s11655-020-3421-y.
[28] M. Vulin, Y. Zhong, B.J. Maloney, B. Bauer, A.M.S. Hartz, Proteasome inhibition protects blood-brain barrier P-glycoprotein and lowers Abeta brain levels in an Alzheimer's disease model, Fluids Barriers CNS 20 (2023) 70, https://doi.org/10.1186/s12987-023-00470-z.
[29] L. Bi, et al., Paris saponin H inhibits the proliferation of glioma cells through the A1 and A3 adenosine receptor-mediated pathway, Int. J. Mol. Med. 47 (2021), https://doi.org/10.3892/ijmm.2021.4863.
[30] H. Sawaoka, et al., Cyclooxygenase-2 inhibitors suppress the growth of gastric cancer xenografts via induction of apoptosis in nude mice, Am. J. Physiol. 274 (1998) G1061–G1067, https://doi.org/10.1152/ajpgi.1998.274.6.G1061.
[31] E. Karatzas, et al., ChemBioServer 2.0: an advanced web server for filtering, clustering and networking of chemical compounds facilitating both drug discovery and repurposing, Bioinformatics 36 (2020) 2602–2604, https://doi.org/10.1093/bioinformatics/btz976.
[32] S. Akhtar, et al., Guggulsterone induces apoptosis in multiple myeloma cells by targeting high mobility group box 1 via janus activated kinase/signal transducer and activator of transcription pathway, Cancers 14 (2022), https://doi.org/10.3390/cancers14225621.
[33] H. Li, et al., PARP inhibitor resistance: the underlying mechanisms and clinical implications, Mol. Cancer 19 (2020) 107, https://doi.org/10.1186/s12943-020-01227-0.
[34] L.D. Fricker, Proteasome inhibitor drugs, Annu. Rev. Pharmacol. Toxicol. 60 (2020) 457–476, https://doi.org/10.1146/annurev-pharmtox-010919-023603.
[35] A.K. Stewart, et al., Carfilzomib, lenalidomide, and dexamethasone for relapsed multiple myeloma, N. Engl. J. Med. 372 (2015) 142–152, https://doi.org/10.1056/NEJMoa1411321.
[36] E. Thorp, D. Cui, D.M. Schrijvers, G. Kuriakose, I. Tabas, Mertk receptor mutation reduces efferocytosis efficiency and promotes apoptotic cell accumulation and plaque necrosis in atherosclerotic lesions of apoe-/- mice, Arterioscler. Thromb. Vasc. Biol. 28 (2008) 1421–1428, https://doi.org/10.1161/ATVBAHA.108.167197.
[37] B.S. Moore, A.S. Eustaquio, R.P. McGlinchey, Advances in and applications of proteasome inhibitors, Curr. Opin. Chem. Biol. 12 (2008) 434–440, https://doi.org/10.1016/j.cbpa.2008.06.033.
[38] S.M. Bair, J.D. Brandstadter, E.C. Ayers, E.A. Stadtmauer, Hematopoietic stem cell transplantation for blood cancers in the era of precision medicine and immunotherapy, Cancer 126 (2020) 1837–1855, https://doi.org/10.1002/cncr.32659.
[39] S.A. Minnie, G.R. Hill, Immunotherapy of multiple myeloma, J. Clin. Invest. 130 (2020) 1565–1575, https://doi.org/10.1172/JCI129205.
[40] A.J. Cowan, et al., Diagnosis and management of multiple myeloma: a review, JAMA 327 (2022) 464–477, https://doi.org/10.1001/jama.2022.0003.
[41] A.L. Garfall, New biological therapies for multiple myeloma, Annu. Rev. Med. 75 (2024) 13–29, https://doi.org/10.1146/annurev-med-050522-033815.

[42] B. Bruno, L. Giaccone, M. Rotta, K. Anderson, M. Boccadoro, Novel targeted drugs for the treatment of multiple myeloma: from bench to bedside, Leukemia 19 (2005) 1729–1738, https://doi.org/10.1038/sj.leu.2403905.
[43] J.F. San-Miguel, M.V. Mateos, Can multiple myeloma become a curable disease? Haematologica 96 (2011) 1246–1248, https://doi.org/10.3324/haematol.2011.051169.
[44] V. Pinto, et al., Multiple myeloma: available therapies and causes of drug resistance, Cancers 12 (2020), https://doi.org/10.3390/cancers12020407.
[45] H. Li, et al., Phase I dose-escalation and expansion study of PARP inhibitor, fluzoparib (SHR3162), in patients with advanced solid tumors, Chin. J. Cancer Res. 32 (2020) 370–382, https://doi.org/10.21147/j.issn.1000-9604.2020.03.08.
[46] J. Luo, et al., Fluzoparib increases radiation sensitivity of non-small cell lung cancer (NSCLC) cells without BRCA1/2 mutation, a novel PARP1 inhibitor undergoing clinical trials, J. Cancer Res. Clin. Oncol. 146 (2020) 721–737, https://doi.org/10.1007/s00432-019-03097-6.
[47] A. Alhusaini, A. Cannon, S.G. Maher, J.V. Reynolds, N. Lynam-Lennon, Therapeutic potential of PARP inhibitors in the treatment of gastrointestinal cancers, Biomedicines 9 (2021), https://doi.org/10.3390/biomedicines9081024.
[48] A. Lee, Fuzuloparib: first approval, Drugs 81 (2021) 1221–1226, https://doi.org/10.1007/s40265-021-01541-x.
[49] L. Wang, et al., Pharmacologic characterization of fluzoparib, a novel poly(ADP-ribose) polymerase inhibitor undergoing clinical trials, Cancer Sci. 110 (2019) 1064–1075, https://doi.org/10.1111/cas.13947.
[50] D.H. Lee, A.L. Goldberg, Proteasome inhibitors: valuable new tools for cell biologists, Trends Cell Biol. 8 (1998) 397–403, https://doi.org/10.1016/s0962-8924(98)01346-4.
[51] K.B. Hendil, The 19 S multicatalytic "prosome" proteinase is a constitutive enzyme in HeLa cells, Biochem. Int. 17 (1988) 471–477.
[52] K.R. Landis-Piwowar, et al., The proteasome as a potential target for novel anticancer drugs and chemosensitizers, Drug Resist Updat 9 (2006) 263–273, https://doi.org/10.1016/j.drup.2006.11.001.
[53] B.A. Teicher, G. Ara, R. Herbst, V.J. Palombella, J. Adams, The proteasome inhibitor PS-341 in cancer therapy, Clin. Cancer Res. 5 (1999) 2638–2645.
[54] M.A. Dimopoulos, P.G. Richardson, P. Moreau, K.C. Anderson, Current treatment landscape for relapsed and/or refractory multiple myeloma, Nat. Rev. Clin. Oncol. 12 (2015) 42–54, https://doi.org/10.1038/nrclinonc.2014.200.
[55] G. Heynen, et al., SUMOylation inhibition overcomes proteasome inhibitor resistance in multiple myeloma, Blood Adv 7 (2023) 469–481, https://doi.org/10.1182/bloodadvances.2022007875.
[56] X. Luo, W.L. Kraus, On PAR with PARP: cellular stress signaling through poly(ADP-ribose) and PARP-1, Genes Dev. 26 (2012) 417–432, https://doi.org/10.1101/gad.183509.111.
[57] E.E. Alemasova, O.I. Lavrik, Poly(ADP-ribosyl)ation by PARP1: reaction mechanism and regulatory proteins, Nucleic Acids Res. 47 (2019) 3811–3827, https://doi.org/10.1093/nar/gkz120.
[58] T. Kamaletdinova, Z. Fanaei-Kahrani, Z.Q. Wang, The enigmatic function of PARP1: from PARylation activity to PAR readers, Cells 8 (2019), https://doi.org/10.3390/cells8121625.